

# Front propagation sustained by additive noise

M. G. Clerc, C. Falcón,\* and E. Tirapegui

Departamento de Física, Facultad de Ciencias Físicas y Matemáticas, Universidad de Chile, Casilla 487-3, Santiago, Chile

The effect of noise in a motionless front between a periodic spatial state and an homogeneous one is studied. Numerical simulations show that noise induces front propagation. From the subcritical Swift-Hohenberg equation with noise, we deduce an adequate equation for the envelope and the core of the front. The equation of the core of the front is characterized by an asymmetrical periodic potential plus additive noise. The conversion of random fluctuations into direct motion of the core of the front is responsible of the propagation. We obtain an analytical expression for the velocity of the front, which is in good agreement with numerical simulations.

## I. INTRODUCTION

The description of macroscopic matter—i.e., matter composed of a large number of microscopic constituents—is usually done using a small number of coarse-grained or macroscopic variables. When spatial inhomogeneities are considered these variables are spatiotemporal fields whose evolution is determined by deterministic partial differential equations (PDEs). This reduction is possible due to a separation of time and space scales, which allows a description in terms of the slowly varying macroscopic variables, which are in fact fluctuating variables due to the elimination of a large number of fast variables whose effect can be modeled including suitable stochastic terms, *noise*, in the PDE. The influence of noise in nonlinear systems has been the subject of intense experimental and theoretical investigations in the last decades [1–17]. Far from being merely a perturbation to the idealized deterministic evolution or an undesirable source of randomness and disorganization, noise can induce specific and even counterintuitive dynamical behavior. The most well-known examples in zero-dimensional systems are noise-induced transitions [1,7,9] and stochastic resonance (see the review in [2] and references therein). More recently, examples in spatially extended system were found, such as, noise-induced phase transitions [3–5,12], noise-induced patterns [13–15], stochastic spatiotemporal intermittency [16], and noise-induced traveling waves [17]. Here, we present another robust effect of noise in extended systems: *the motion of a static front connecting a stable homogeneous state with a stable inhomogeneous (spatially periodic) state due to additive noise*. A first preliminary discussion of this effect was done by the present authors in a recent Letter [18], and the aim of this article is to study and characterize the universal mechanism which is at the origin of the front motion in the presence of noise.

The concept of front propagation emerged in the field of population dynamics [19], and the interest in this type of problems has been growing steadily in chemistry, physics, and mathematics. In physics, front propagation plays a central role in a large variety of situations, ranging from reaction

diffusion models, to general pattern-forming systems (see the review in [20] and references therein). A front solution is a solution which links spatially two extended states. One of the most studied front solutions is the front connecting a stable uniform state with an unstable one: the Fisher-Kolmogorov-Petrovsky-Piskunov (FKPP) front [21]. The speed of propagation of this type of front is not unique, and it is fixed by the initial conditions [22]. Another well-known type of front, the *normal front*, connects two stable uniform states. The speed of this kind of front is unique, and for a variational system it is proportional to the difference of free energy between the two uniform states. In Fig. 1 the dashed curve represents the typical behavior of the speed of a normal front as a function of an arbitrary parameter. Note that the speed of the front is zero only at the Maxwell point where both states have the same energy. This picture is modified when one considers a front connecting an spatially periodic state with a uniform one, which is the case of interest for us here. In this case the speed is zero not only in one point but in a whole interval of variation of the relevant parameter, the *pinning range* [23], and additive noise will induce front motion [18]. In Fig. 1 the solid line represents the typical speed of these fronts and the

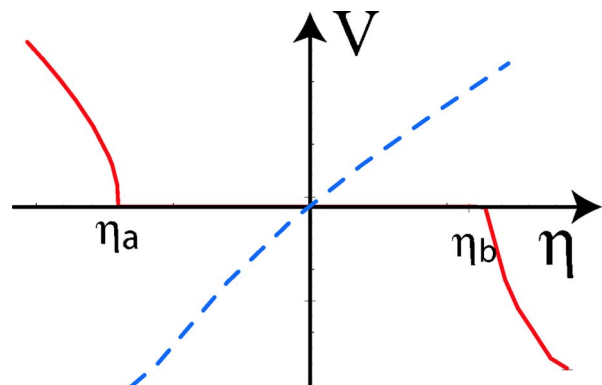


FIG. 1. (Color online) Speed of the front as function of one parameter. The dashed curve depicts the typical behavior of the speed of a normal front as function of arbitrary parameter, and the solid curve represents the speed of a front that links a spatial periodic state and uniform one. For the sake of simplicity the origin represents the Maxwell point. The pinning range is depicted by the interval between  $\eta_a$  and  $\eta_b$ .

\*Present address: Laboratoire de Physique Statistique, École Normale Supérieure, 24 rue Lhomond, 75231 Paris Cedex 05, France.

interval  $[\eta_a, \eta_b]$  represents the pinning range. The effect of additive noise on the speed of a “normal front” is just a random fluctuation of its speed. On the other hand, the influence of multiplicative noise in a front, which will not occupy us in this paper, has been extensively studied in the literature, particularly concerning the issue of velocity selection [24].

The paper is organized as follows. In Sec. II, we present several examples of numerical observations of motion of fronts induced by additive noise. In Sec. III, we use a prototype model which exhibits this type of front to derive an adequate equation for the envelope of the front solution: an amended amplitude equation, which includes a resonant term coming from the additive noise whose origin is discussed in Appendix A and also nonresonant terms. It turns out that the contributions of the noise and of the nonresonant terms are of the same kind, giving rise to an asymmetric potential with denumerable stable equilibria in the equation for the core of the front which is derived in Sec. IV. In this equation the dominant contribution to the potential near threshold comes from the noise term. In Sec. V, we obtain an analytical expression for the mean velocity of the front using Dinkyn’s equation, which is proportional to Kramer’s rate in the weak-noise limit. This expression is in good agreement with numerical simulations. In Sec. VI, we summarize our results. In Appendix A, we show that, as stated and used in the text in Sec. III, noise is always resonant in the sense of the *stochastic* normal form. In Appendix B, we give the technical details involved in the derivation of the equation for the core of the front. And finally in Appendix C, we show that the mean value of the derivative of the phase remains bounded, which is a necessary consistency condition of our approach.

## II. NUMERICAL OBSERVATIONS OF ADDITIVE NOISE-INDUCED FRONT PROPAGATION

In order to illustrate the generic nature of additive noise-induced front propagation, we consider the effect of additive noise over several dynamical systems which have fronts linking a spatially periodic solution and a uniform one.

(a) *Lifshitz normal form.* A prototype model that exhibits coexistence of a spatially periodic solution and a uniform state is the Lifshitz normal form [25]

$$\begin{aligned} \partial_t u = & \eta + \mu u - u^3 + \nu \partial_{xx} u - \partial_{xxx} u + d u \partial_{xx} u + c (\partial_x u)^2 \\ & + \sqrt{\Delta} \zeta(x, t) \end{aligned} \quad (1)$$

This model describes the dynamics close to the confluence of a bistability of homogeneous states and a spatial bifurcation—that is, near a critical point of codimension 3, called a Lifshitz point. Here,  $\mu$  is the bifurcation parameter,  $\eta$  accounts for the asymmetry between the two homogeneous states, and the term  $\partial_{xxx} u$  describes a superdiffusion, accounting for the short-distance repulsive interaction, whereas the terms proportional to  $d$  and  $c$  are, respectively, the nonlinear diffusion and convection,  $\zeta(x, t)$  is a Gaussian white noise with zero mean value and correlation  $\langle \zeta(x, t) \zeta(x', t') \rangle = \delta(x-x') \delta(t-t')$ , and  $\Delta$  represents the intensity of the noise. Recently, this model has been used to describe the complex dynamics observed in a liquid-crystal light valve with optical

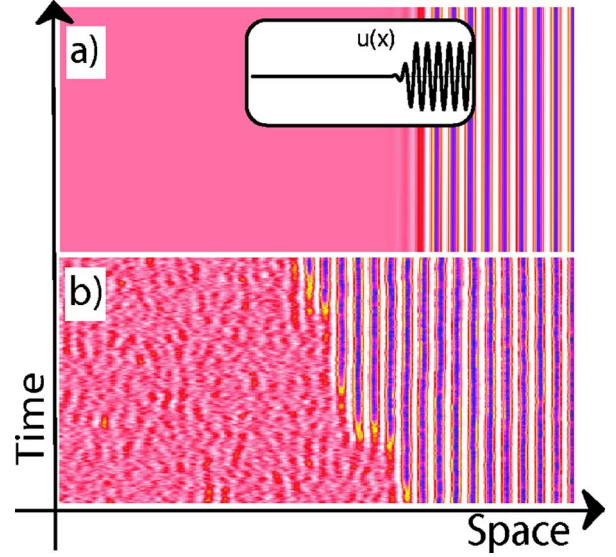


FIG. 2. (Color online) Spatiotemporal evolution of Eq. (1), with time running up. The gray scale is proportional to field  $u$ . The inset is the initial condition. The parameters have been chosen as  $\eta = -0.044$ ,  $\mu = -0.0126$ ,  $\nu = -1.0$ ,  $c = 0.177$ , and  $d = 0.2$  (a)  $\delta = 0.0$ , and (b)  $\delta = 0.9$ .

feedback [25]. In the region corresponding to the pinning range of the above model, the system exhibits a motionless front that connects the spatially periodic state with the uniform one [cf. Fig. 2(a)]. When we consider the effect of additive noise, we notice that it induces the invasion of one of the states over the other one, or vice versa, depending on the region of parameters we initially choose. This situation is depicted in Fig. 2.

(b) *Population dynamics.* In order to take into account the long-range effect of the environment one can consider non-local models to describe the population dynamics. In this type of models the emergence of self-organized structures and patterns is well known [26,27]. A minimal model that exhibits the coexistence of a spatial periodic state and a uniform one is the variational nonlocal Nagumo model [28].

$$\begin{aligned} \partial_t u(x, t) = & \partial_{xx} u + u(\alpha - u)(1 - u) + u^3 \\ & - u(x, t) \int_{\Omega} u(x', t)^2 f_{\sigma}(x, x') d^2 x', \end{aligned} \quad (2)$$

where  $u(x, t)$  is the local density and  $\alpha$  is the adversity parameter which accounts for the complications of development of the species under study. The adversity characterizes the equilibrium point and can always be chosen to satisfy  $0 \leq \alpha \leq 1$  without loss of generality. The function  $f_{\sigma}(x, x')$  is the influence function, characterized by a range  $\sigma$  and normalized in the domain  $\Omega$  under study. For simplicity, we consider the environment to be homogeneous and isotropic. Then  $f_{\sigma}(x, x') = f_{\sigma}(x - x')$ , with  $f_{\sigma}(z)$  even, and  $\int_{\Omega} f_{\sigma}(x, x') dx' = 1$ . In the extreme local limit  $\sigma \rightarrow 0$ , one has  $f_{\sigma}(x, x') = \delta(x - x')$ , and Eq. (2) reduces to the Nagumo model [26]. Let us now consider the simple influence functions  $f_{\sigma}(z) = \theta(\sigma + z) \theta(\sigma - z) / 2\sigma$ , where  $\theta(z)$  is the Heaviside func-

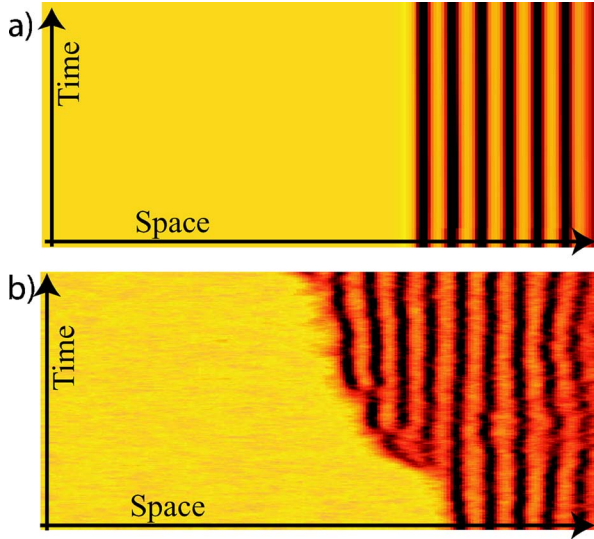


FIG. 3. (Color online) Spatiotemporal evolution the population density  $u(x,t)$  for the model (2), with time running up,  $\alpha=0.35$ ,  $\sigma=4\%$  of total system size, system size=400 points, (a) without noise, and (b) with additive noise. The gray scale is proportional to the population density.

tion. The dynamics is described by the parameters  $\{\alpha, \sigma$  and Eq. (2) can be written as

$$\partial_t u = - \frac{\delta \mathcal{F}[u]}{\delta u},$$

where the Lyapunov functional  $\mathcal{F}[u]$  has the form

$$\mathcal{F}[u] = \int_{\Omega} \left\{ \frac{1}{2} (\partial_x u)^2 + \frac{\alpha}{2} u^2 - \frac{(\alpha+1)}{3} u^3 \right\} dx + \frac{1}{4} \int_{\Omega} \int_{\Omega} u^2 u'^2 f_{\sigma}(x, x') dx dx'.$$

Hence, the dynamics of model (2) is of the relaxation type and the stationary states are local minima of  $\mathcal{F}[u]$ .

The model (2) exhibits a motionless front that connects the spatially periodic state with the uniform one [cf. Fig. 3(a)]. Note that these motionless front solutions are not the global minimum of the Lyapunov functional  $\mathcal{F}[u]$ ; however, they are local minima of this functional and the population only can spread if one adds energy to the system. For instance, if we consider the effect of additive noise, the periodic population state can invade the unpopulated state ( $u=0$ ). In Fig. 3, we depict the spread of population due to the presence of additive noise in the variational nonlocal Nagumo model.

(c) *Subcritical Swift-Hohenberg equation.* A prototype model used in pattern-forming system is the Swift-Hohenberg equation [20]. Initially, this model was used to describe the onset of Rayleigh-Bénard convection [20]. From the point of view of dynamical systems theory, this model describes the confluence of a subcritical stationary and a spatial bifurcation. Generalizations of this model have been used intensively to account for pattern formation in several sys-

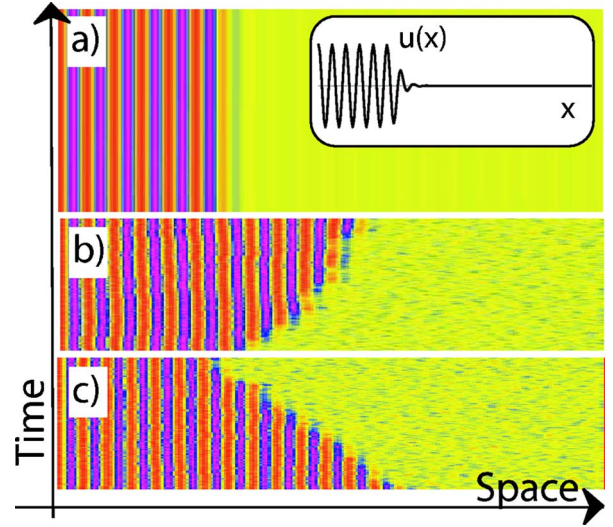


FIG. 4. (Color online) Spatiotemporal evolution of Eq. (3), with time running up. The gray scale is proportional to field  $u$ . The inset is the initial condition. The parameters have been chosen as  $\nu=1.0$ ,  $q=0.7$ , (a)  $\epsilon=-0.16$  and  $\eta=0.0$ , (b)  $\epsilon=-0.16$  and  $\eta=0.4$ , and (c)  $\epsilon=-0.177$  and  $\eta=-0.16$ .

tems (see the review in [20] and reference therein). We shall consider here the subcritical Swift-Hohenberg equation, which exhibits the coexistence between a uniform state and an spatially periodic one. In the presence of additive noise this equation reads

$$\partial_t u = \varepsilon u + \nu u^3 - u^5 - (\partial_{xx} + q^2)u + \sqrt{\eta} \zeta(x,t), \quad (3)$$

where  $u(x,t)$  is an order parameter,  $\varepsilon - q^4$  is the bifurcation parameter,  $q$  is the wave number of the periodic spatial solution,  $\nu$  is the control parameter of the type of bifurcation (supercritical or subcritical),  $\zeta(x,t)$  is a Gaussian white noise with zero mean value and correlation  $\langle \zeta(x,t) \zeta(x',t') \rangle = \delta(x-x') \delta(t-t')$ , and  $\eta$  represents the intensity of the noise. In the pinning range of the model above the system exhibits a motionless front that connects the spatially periodic state with the uniform one [cf. Fig. 4(a)]. When one considers the effect of additive noise, depending where is the control parameter inside the pinning range, it induces on average that one of the states invades the other one. This situation is shown in Fig. 4, and in Fig. 5 we show the speed of the front of this model (3) with and without additive noise.

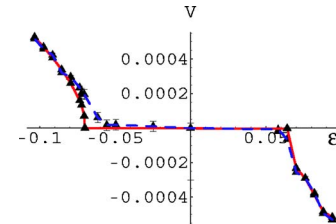


FIG. 5. (Color online) Mean velocity of the front with and without noise. The thick and dashed curves are the average velocity of the front of Eq. (3) for  $\varepsilon=-0.16$ ,  $\nu=1.0$ ,  $q=0.7$ ,  $\eta=0.0$ , and  $\eta=0.01$ , respectively.

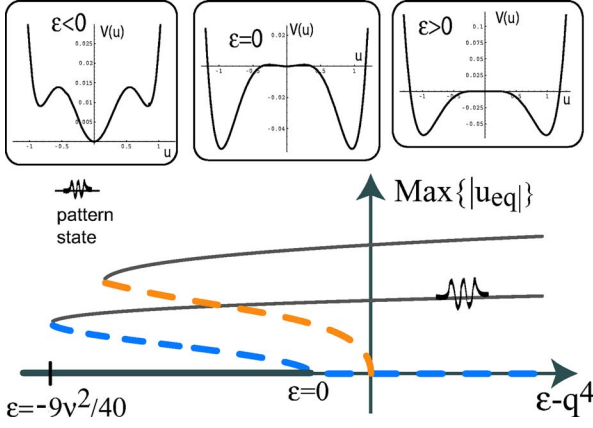


FIG. 6. (Color online) Bifurcation diagram of the subcritical Swift-Hohenberg model (3); the horizontal axis represents the control parameter and the vertical one represents the maximum value of the absolute value of the equilibrium state. As solid lines are depicted the stable states and as dashed lines the unstable ones. The model (3) exhibits the coexistence between two uniform states and spatial periodic one. In the insets are illustrated the local potentials  $V(u)$  for negative, zero, and positive  $\epsilon$ , respectively.

In brief, we have considered three different dynamical systems, which exhibit a motionless front solution linking a spatially periodic state and a uniform one. When additive noise is taken into account generically one state starts to invade the other one by means of a noise-induced front propagation. In order to figure out the mechanism of this propagation in the next section we shall study in detail the dynamics of the subcritical Swift-Hohenberg equation with additive noise at the onset of spatial instability.

### III. AMPLITUDE EQUATION AND EVOLUTION OF THE CORE OF THE FRONT

In order to understand the mechanism through which additive noise induces front propagation, we consider a prototype model that exhibits this type of front, the *subcritical Swift-Hohenberg equation with noise*, Eq. (3). This model reads

$$\partial_t u = -\frac{\delta \mathcal{F}}{\delta u} + \sqrt{\eta} \zeta'(x, t), \quad (4)$$

where the free energy has the form

$$\mathcal{F} = \int dx \left\{ -\frac{(\epsilon - q^4)u^2}{2} - \frac{\nu u^4}{4} + \frac{u^6}{6} - q^2(\partial_x u)^2 - \frac{(\partial_{xx} u)^2}{2} \right\}.$$

Hence, the dynamics of the above model is characterized by the minimization of this free energy. In Fig. 6, we show the typical bifurcation diagram observed in the subcritical Swift-Hohenberg model. Note that the system exhibits coexistence between different homogeneous states and the spatial periodic one. For small  $\epsilon$  and  $\mu$ , the system shows spatially periodic solutions with small amplitude (proportional to  $\sqrt{\nu}$ ), and consequently the amplitude equation will be an adequate framework for our study. The free energy has a local potential

$$V(u) = -\frac{(\epsilon - q^4)u^2}{2} - \frac{\nu u^4}{4} + \frac{u^6}{6},$$

which characterizes the stability properties of the uniform states.

#### A. Amplitude equation

In the limit of small  $\nu$ , we look for a solution  $u(x, t)$  in Fourier modes putting  $u = A_0 e^{iqx} + \bar{A}_0 e^{-iqx} + \dots$ , with  $A_0$  of order  $\nu^{1/2}$ . Replacing in the subcritical Swift-Hohenberg equation (3), we find that  $A_0$  satisfies

$$\epsilon A_0 + 3\nu |A_0|^2 A_0 - 10 |A_0|^4 A_0 = 0. \quad (5)$$

For small and negative  $\nu$  and  $-9\nu^2/40 < \epsilon < 0$  (cf. Fig. 6), the system exhibits coexistence between a stable homogenous state  $u=0$  and a periodic spatial one:  $u = \sqrt{\nu} \{ \sqrt{2(1 + \sqrt{1 + 40\epsilon/9\nu})} \cos[q(x - x_0)] \} + o(\nu^{5/2})$ , where  $x_0$  is an arbitrary number, related to the symmetry of translation. In this region of the space of parameters, we find then a front solution between these two states. This type of solution is a heteroclinic curve of the spatial dynamical system ( $\partial_t u = 0$ ) associated with the above model [29]. A front between an homogeneous and a spatially oscillating state can be described by an envelope  $A(X, T)$ , which is introduced through the ansatz

$$u = A(X = |\epsilon|^{1/2} x, T = |\epsilon| t) e^{iqx} + \text{c.c.} + W(X, T), \quad (6)$$

where  $W(X, T)$  is a small function of the order of  $\nu^{5/2}$ ,  $A \sim \nu^{1/2}$ , and  $\nu \sim |\epsilon|^{1/2}$ . Introducing the above ansatz in Eq. (3), linearizing in  $W$ , and considering the dominating order ( $\nu^{5/2}$ ), we obtain

$$\begin{aligned} (\partial_x^2 + q^2)^2 W = & (\epsilon A + 3\nu |A|^2 A - 10 |A|^4 A) e^{iqx} (4|\epsilon| q^2 \partial_{XX} A \\ & - |\epsilon| \partial_T A) e^{iqx} + (\nu A^3 - 5 |A|^2 A^3) e^{i3qx} - A^5 e^{4iqx} \\ & + \frac{\sqrt{\eta}}{2} \zeta'(x, t) e^{-iqx} + \text{c.c.}, \end{aligned}$$

where the self-adjoint operator  $L = (\partial_x^2 + q^2)^2$  has a nontrivial kernel characterized by the eigenfunctions  $\{e^{iqx}, e^{-iqx}\}$ . Taking  $W=0$  at this order we obtain an equation for  $A(X, t)$  which contains nonresonant terms

$$\begin{aligned} \partial_t A(X, t) = & \left[ \epsilon A + 3\nu |A|^2 A - 10 |A|^4 A + 4|\epsilon| q^2 \partial_{XX} A \right. \\ & \left. + \frac{\sqrt{\eta}}{2} \zeta'(x, t) e^{-iqx} \right] + (\nu A^3 - 5 A^4 \bar{A}) e^{2iqx} - A^5 e^{4iqx}. \end{aligned}$$

In this equation the terms in square brackets  $[\dots]$ , except the noise term, are the ones in the usual normal form, which is obtained from the solvability condition for  $W$  in the previous equations—i.e., that the right-hand side is orthogonal to the kernel  $L = (\partial_x^2 + q^2)^2$ . The noise term is included there since it is always resonant in the sense that it cannot be removed by

a stochastic nonlinear and nonsingular close to the identity change of variables as we discuss in Appendix A following Refs. [33–37], and the rest of the terms are the nonresonant terms up to this order which can be eliminated by a deterministic nonlinear and nonsingular close to the identity change of variables. Defining

$$A(x, t) = \sqrt{\frac{3\nu}{10}} B(y, \tau), \quad x = \frac{2\sqrt{10}q}{3\nu} y, \quad t = \frac{10}{9\nu^2} \tau,$$

the envelope equation reads

$$\begin{aligned} \partial_\tau B(y, \tau) = & \sigma B + B|B|^2 - B|B|^4 + \partial_{yy} B \\ & + \left( \frac{1}{9\tilde{\nu}} B^3 - \frac{1}{2} B^4 \bar{B} \right) e^{2iqy/\alpha\sqrt{|\varepsilon|}} - \frac{1}{10} B^5 e^{2iqy/\alpha\sqrt{|\varepsilon|}} \\ & + \frac{\beta\sqrt{\eta}}{2\alpha|\varepsilon|^2} e^{-iqy/\alpha\sqrt{|\varepsilon|}} \zeta(y, \tau), \end{aligned} \quad (7)$$

where the new noise  $\zeta$  is proportional to  $\zeta'$  and has mean value zero and correlation  $\langle \zeta(y, \tau) \zeta(y', t') \rangle = \delta(y-y') \delta(t-t')$ . One has

$$\sigma = \frac{10\varepsilon}{9\nu^2}, \quad \nu = \sqrt{|\varepsilon|} \tilde{\nu}, \quad \alpha = \frac{3\tilde{\nu}}{2\sqrt{10}q}, \quad \beta = \frac{10^{1/4} 10^2}{81\tilde{\nu}^4}.$$

If in the above amplitude equation we eliminate all the terms with an explicit dependence on the spatial variable  $y$ , we obtain the normal form without noise:

$$\partial_\tau B(y, \tau) = \sigma B + B|B|^2 - B|B|^4 + \partial_{yy} B = - \frac{\delta F[B, \bar{B}]}{\delta \bar{B}}, \quad (8)$$

which is variational, as indicated, with the functional

$$F[B, \bar{B}] = - \int dy \left[ \sigma |B|^2 + \frac{1}{2} |B|^4 - \frac{1}{3} |B|^6 - |\partial_y B|^2 \right].$$

By minimizing this free energy functional, we find that the system has five **uniform states**, three of which are stable:  $B=0$  and  $B_\pm = \pm \sqrt{(1 + \sqrt{1+4\sigma})/2}$  (cf. Fig. 6). It is then straightforward to show that the previous equation (the normal form without noise) has front solutions connecting two homogeneous stable states,  $B=0$  and  $B=B_\pm = \pm \sqrt{(1 + \sqrt{1+4\sigma})/2}$ , when  $-\frac{1}{4} \leq \sigma < 0$ , and these fronts will be stationary only when the free energy for both states is the same—i.e., when the system is in the Maxwell point. As already stated all the terms which were eliminated to arrive at Eq. (8) are nonresonant (except the noise term), in the sense that they can be eliminated by a nonlinear and nonsingular change of variables near the bifurcation point [33], and hence are usually neglected. As we shall see these terms can give an explanation to the locking phenomena and the pinning range [31]. Nevertheless, it should be pointed out that if we include only the noise term which is always resonant [34–37] (Appendix A), this would be enough to explain the locking phenomena, the pinning range, and the motion of the front, since this term

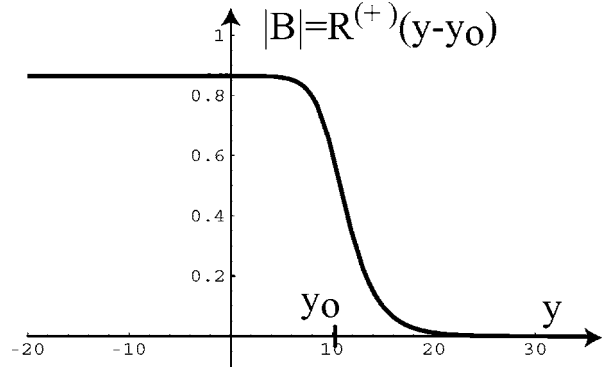


FIG. 7. Motionless front solution of Eq. (8), computed at the Maxwell point. As the vertical axis is represented the modulus of amplitude  $B$  as a function of the position.  $y_0$  represents the position of the core of the front.

dominates the similar terms coming from the nonresonant terms near the bifurcation point [see Eq. (12)]. The nonresonant terms and the noise term give exponentially small contributions due to the fast oscillating exponentials and can be treated perturbatively in the amplitude equation.

We can calculate the Maxwell point from  $F[B, \bar{B}]$ , and we obtain  $\sigma_M = -3/16$ . We put now  $\sigma = \sigma_M + \delta\sigma$  in the complete equation for  $B(y, \tau)$ , which we treat as the variational part in the Maxwell point plus small terms which can be treated as perturbations. One has

$$\begin{aligned} \partial_\tau B(y, \tau) = & \left( -\frac{3}{16} B + B|B|^2 - B|B|^4 + \partial_{yy} B \right) \\ & + \left\{ \delta\sigma B + \left( \frac{1}{9\tilde{\nu}} B^3 - \frac{1}{2} B^4 \bar{B} \right) e^{2iqy/\alpha\sqrt{|\varepsilon|}} \right. \\ & \left. - \frac{1}{10} B^5 e^{4iqy/\alpha\sqrt{|\varepsilon|}} + \frac{\beta\sqrt{\eta}}{2|\varepsilon|^2} e^{-iqy/\alpha\sqrt{|\varepsilon|}} \zeta(y, \tau) \right\}, \end{aligned}$$

where the small terms are inside the curly brackets  $\{\dots\}$  and they include the noise term. The unperturbed equation for  $B(y, \tau)$  at the Maxwell point has the exact stationary front solutions

$$B^{(\pm)}(y - y_0) = R_0^{(\pm)}(y - y_0) e^{i\varphi},$$

where  $\varphi$  is an arbitrary constant phase,  $y_0$  stands for the position of the core of the front, and  $R_0^{(\pm)}(y - y_0)$  is given by

$$R_0^{(\pm)}(y - y_0) = \sqrt{\frac{3/4}{1 + e^{\pm\sqrt{3/4}(y-y_0)}}}.$$

From now on, we shall work with the front  $R_0^{(+)}(y - y_0)$  which goes from zero at  $y = -\infty$  to the value  $\sqrt{3/4}$  at  $y = +\infty$  and we shall simply write  $R_0$  for this solution which is depicted in Fig. 7. We put  $B(y, \tau) = R(y, \tau) e^{i\Theta(y, \tau)}$  in the complete equation for  $B(y, \tau)$ , and we obtain

$$\begin{aligned}
& \partial_\tau R(y, \tau) + i\partial_\tau \Theta(y, \tau) R(y, \tau) \\
&= \left( -\frac{3}{16} R + R^3 - R^5 + \partial_{yy} R \right) \\
&+ [2i\partial_y R \partial_y \Theta + iR \partial_{yy} \Theta - R(\partial_y \Theta)^2] \\
&+ \left\{ \delta\sigma R + \left( \frac{1}{9\tilde{\nu}} R^3 e^{2i\Theta} - \frac{1}{2} R^5 e^{4i\Theta} \right) e^{2iqy/\alpha\sqrt{|\varepsilon|}} \right. \\
&\left. - \frac{1}{10} R^5 e^{4i\Theta} e^{4iqy/\alpha\sqrt{|\varepsilon|}} + \frac{\beta\sqrt{\eta}}{2|\varepsilon|^2} e^{-iqy/\alpha\sqrt{|\varepsilon|}} \zeta(y, \tau) \right\}.
\end{aligned}$$

### B. Nonresonant terms

In order to solve the above equation we make the ansatz

$$R(y, \tau) = R_0[y - y_0(\tau)] + \tilde{\varepsilon}\rho(y, y_0(\tau)),$$

$$\Theta(y, \tau) = \tilde{\varepsilon}\Theta_1(y, y_0(\tau)),$$

where  $\tilde{\varepsilon}$  is a small parameter, and we have promoted the coordinate  $y_0$  of the core of the front to a function of time  $y_0(\tau)$ . We replace our ansatz in the previous equation, where we assume that the small terms in the square brackets are  $O(\tilde{\varepsilon})$  as well as the time derivative  $dy_0(\tau)/d\tau \equiv \dot{y}_0$ , and we equate the real and imaginary parts at  $O(\tilde{\varepsilon})$ , obtaining the equations

$$\begin{aligned}
& -R_{0y}(y - y_0(\tau))\dot{y}_0 \\
&= \tilde{\varepsilon}L(y - y_0)\rho + \delta\sigma R_0(y - y_0(\tau)) \\
&+ \left( \frac{1}{9\tilde{\nu}} R_0^3 - \frac{1}{2} R_0^5 \right) \cos\left( 2q \frac{y}{\alpha\sqrt{|\varepsilon|}} \right) \\
&- \frac{1}{10} R_0^5 \cos\left( 4q \frac{y}{\alpha\sqrt{|\varepsilon|}} \right) + \frac{\beta\sqrt{\eta}}{2|\varepsilon|^2} \cos\left( q \frac{y}{\alpha\sqrt{|\varepsilon|}} \right) \zeta(y, \tau)
\end{aligned} \tag{9}$$

and

$$\begin{aligned}
& \frac{d}{dy} [R_0(y - y_0(\tau))^2 \Theta_{1y}] \\
&= - \left( \frac{1}{9\tilde{\nu}} R_0^4 - \frac{1}{2} R_0^6 \right) \sin\left( 2q \frac{y}{\alpha\sqrt{|\varepsilon|}} \right) - \frac{1}{10} R_0^6 \sin\left( 4q \frac{y}{\alpha\sqrt{|\varepsilon|}} \right) \\
&- \frac{\beta\sqrt{\eta}}{2|\varepsilon|^2} R_0(y - y_0(\tau)) \sin\left( q \frac{y}{\alpha\sqrt{|\varepsilon|}} \right) \zeta(y, \tau),
\end{aligned} \tag{10}$$

where

$$R_{0y}(y) \equiv \frac{dR_0}{dy}, \quad R_{0yy}(y) \equiv \frac{d^2R_0}{dy^2}, \quad \Theta_{1y} \equiv \partial_y \Theta_1(y, y_0(\tau))$$

and

$$L(y - y_0) \equiv -\frac{3}{16} + 3R_0(y - y_0)^2 - 5R_0^4 + \partial_{yy}$$

is the operator obtained through linearization of the variational equation for  $B(y, \tau)$  around the front. The function  $R_0(y - y_0(\tau))$  satisfies the equation

$$-\frac{3}{16} R_0 + R_0^3 - R_0^5 + \partial_{yy} R_0 = 0.$$

Taking the derivative with respect to  $y$  one shows

$$L(y - y_0) R_{0y}(y - y_0) = 0.$$

The operator  $L(y - y_0)$  is self-adjoint in the scalar product

$$\{f(y), g(y)\} = \int dy f(y) g^*(y),$$

where  $f(y)^*$  stands for the complex conjugate of  $f(y)$ . We multiply the equation for  $y_0(\tau)$  by  $R_0(y - y_0(\tau))$ , and we integrate over  $y$ . We obtain the solvability condition (putting  $\tilde{\varepsilon} = 1$ )

$$\begin{aligned}
& -\{R_{0y}, R_{0y}\} d_\tau y_0(\tau) \\
&= \{R_{0y}, L\rho\} + \delta\sigma\{R_{0y}, R_0\} \\
&+ \int dy R_{0y}(y - y_0(\tau)) \left( \frac{1}{9\tilde{\nu}} R_0^3 - R_0^5 \right) \cos\left( 2q \frac{y}{\alpha\sqrt{|\varepsilon|}} \right) \\
&- \frac{1}{10} \int dy R_{0y} R_0(y - y_0(\tau))^5 \cos\left( 4q \frac{y}{\alpha\sqrt{|\varepsilon|}} \right) \\
&+ \frac{\beta\sqrt{\eta}}{2|\varepsilon|^2} \int dy R_{0y}(y - y_0(\tau)) \cos\left( q \frac{y}{\alpha\sqrt{|\varepsilon|}} \right) \zeta(y, \tau).
\end{aligned} \tag{11}$$

One has  $\{R_{0y}, R_{0y}\} = 3/4 = 1/a$  and  $\{R_{0y}, R_0\} = 3/8$ . On the other hand, since  $L$  is self-adjoint, one has  $\{R_{0y}, L\rho\} = \{LR_{0y}, \rho\} = 0$  and we obtain an equation for  $y_0(\tau)$  of the form ( $\sqrt{\tilde{\eta}} \equiv a\beta\sqrt{\eta}/2|\varepsilon|^2$ )

$$\dot{y}_0(\tau) = A(y_0(\tau)) - \sqrt{\tilde{\eta}} \int dy R_{0y} \cos\left( q \frac{y}{\alpha\sqrt{|\varepsilon|}} \right) \zeta(y, \tau), \tag{12}$$

with

$$\begin{aligned}
A(y_0(\tau)) &\equiv -\frac{3}{8} a \delta\sigma \\
&+ a \int dy \left[ R_{0y} \left( -\frac{1}{9\tilde{\nu}} R_0^3 + R_0^5 \right) \cos\left( 2q \frac{y}{\alpha\sqrt{|\varepsilon|}} \right) \right] \\
&+ \frac{a}{10} \int dy R_{0y} R_0(y - y_0(\tau))^5 \cos\left( 4q \frac{y}{\alpha\sqrt{|\varepsilon|}} \right).
\end{aligned}$$

In the equation for  $y_0(\tau)$  the product of a function of the stochastic process  $y_0(\tau)$  with the white noise  $\zeta(y, \tau)$  is not defined due to the singular properties of the noise. We define it considering  $\zeta(y, \tau)$  as the limit of a physical noise with time correlation proportional to a symmetric function  $\Delta_\mu(\tau - \tau')$  of width  $\mu$ , where  $\mu$  is much smaller than the characteristic times of variation of the macroscopic physical variables, which tends to  $\delta(\tau - \tau')$  when  $\mu$  tends to zero. This

leads to the Stratonovich interpretation for the undefined product [38]. In Appendix B we show that this gives a supplementary drift which is added to  $A(y_0(\tau))$  and we transform the noise term to obtain (neglecting an exponentially small contribution to the last term)

$$\dot{y}_0(\tau) = A(y_0(\tau)) + \sqrt{\frac{\tilde{\eta}}{2a}} \xi(\tau) - \frac{\tilde{\eta}}{2} \int dy R_{0y} R_{0yy} \cos\left(2q \frac{y}{\alpha\sqrt{|\varepsilon|}}\right),$$

where  $\xi(\tau)$  is a Gaussian white noise of zero mean value and correlation  $\langle \xi(\tau)\xi(\tau') \rangle = \delta(\tau - \tau')$ . If we make the change of variables  $y' = y - y_0(\tau)$  in the last integral and in the integrals in the definition of  $A(y_0(\tau))$ , we obtain the equation (see Appendix B for the calculation)

$$d_\tau y_0(\tau) = -\frac{3}{2} a \delta \sigma \sqrt{K_1^2 + K_2^2} \cos\left(2q \frac{y_0(\tau)}{\alpha\sqrt{|\varepsilon|}} + \phi\right) + \sqrt{\frac{\tilde{\eta}}{2a}} \zeta(\tau) + e^{-c2q/\sqrt{|\varepsilon|}}, \quad (13)$$

where  $c \equiv \sqrt{4\pi/3\alpha}$ . In the last equation  $K_1$  and  $K_2$  are not exponentially small (for small  $|\varepsilon|$ ) and we have neglected a term  $O(e^{-c4q/\sqrt{|\varepsilon|}})$ . We have

$$K_1 = e^{c2q/\sqrt{|\varepsilon|}} \left[ \text{Re}(K) - \frac{9\tilde{\eta}}{128} \frac{q}{\alpha\sqrt{|\varepsilon|}} \text{Im}I \right],$$

$$K_2 = e^{c2q/\sqrt{|\varepsilon|}} \left[ \text{Im}(K) + \frac{9\tilde{\eta}}{128} \frac{q}{\alpha\sqrt{|\varepsilon|}} \text{Re}I \right],$$

$$\cos \phi = \frac{K_1}{\sqrt{(K_1)^2 + (K_2)^2}},$$

$$\sin \phi = \frac{K_2}{\sqrt{(K_1)^2 + (K_2)^2}}, \quad (14)$$

with

$$K = a \int dy \left[ -\frac{1}{9\nu} R_{0y}(y) R_0(y)^3 + \frac{1}{2} R_{0yy}(y) R_0(y)^5 \right] e^{i2qy/\alpha\sqrt{|\varepsilon|}} = O(e^{-c2q/\sqrt{|\varepsilon|}}),$$

and

$$I = \int dy \frac{e^{-2\sqrt{(3/4)y}}}{(1 + e^{-\sqrt{(3/4)y}})^3} e^{i2qy/\alpha\sqrt{|\varepsilon|}} = O(e^{-c2q/\sqrt{|\varepsilon|}}).$$

We have obtained then in Eq. (13) our final equation for the core of the front which tells us that the coordinate  $y_0(\tau)$  of the core is a stochastic diffusion process defined by this equation. In the next section, we shall study Eq. (13) and show that it is at the origin of the motion of the front. We take care now of Eq. (10) which involves the phase  $\Theta_1$ . There is no solvability condition here, and we have then to show that  $\Theta_1$  can be calculated and is bounded. Since

$R_{0y}(y - y_0(\tau))$  vanishes for  $y \rightarrow -\infty$ , we integrate Eq. (10) from  $-\infty$  to  $y$  to obtain

$$R_0(y - y_0(\tau))^2 \Theta_{1y}(y, y_0(\tau)) = \int_{-\infty}^y dy' \left[ -\frac{1}{9\nu} R_0(y' - y_0(\tau))^4 + \frac{1}{2} R_0^6 \right] \sin\left(2q \frac{y'}{\alpha\sqrt{|\varepsilon|}}\right) + \int_{-\infty}^y dy' \frac{1}{10} R_0(y' - y_0(\tau)) \sin\left(4q \frac{y'}{\alpha\sqrt{|\varepsilon|}}\right) + \frac{\sqrt{\tilde{\eta}}}{a} \int_{-\infty}^y dy' R_0(y' - y_0(\tau)) \sin\left(q \frac{y'}{\alpha\sqrt{|\varepsilon|}}\right) \zeta(y', \tau).$$

In the last term of this equation, we have the same problem as in Eq. (11)—i.e., an undefined product of a function of the process  $y_0(\tau)$  with the white noise  $\zeta(y, \tau)$  which we interpret in the Stratonovich sense. After a long calculation done in Appendix C, we obtain

$$R_0(y - y_0(\tau))^2 \Theta_{1y} = -\frac{1}{16\nu} |S^{(1)}(y - y_0(\tau))| \cos\left(2q \frac{y_0(\tau)}{\alpha\sqrt{|\varepsilon|}} - \varphi^{(1)}\right) + \frac{27}{128} |S^{(2)}(y - y_0(\tau))| \cos\left(2q \frac{y_0(\tau)}{\alpha\sqrt{|\varepsilon|}} - \varphi^{(2)}\right) + \frac{27}{640} |S^{(3)}(y - y_0(\tau))| \cos\left(2q \frac{y_0(\tau)}{\alpha\sqrt{|\varepsilon|}} - \varphi^{(3)}\right) - \frac{9\tilde{\eta}}{256a} |I(y - y_0(\tau))| \cos\left(2q \frac{y_0(\tau)}{\alpha\sqrt{|\varepsilon|}} - \varphi\right) + \frac{\sqrt{\tilde{\eta}}}{a} \left[ \int_{-\infty}^y dy' R_0(y' - y_0(\tau)) \times \sin\left(q \frac{y'}{\alpha\sqrt{|\varepsilon|}}\right) \zeta(y', \tau) \right]_{\gamma_1(0)},$$

where  $\gamma_1(0)$  in the noise term means that in a time discretization  $y_0(\tau)$  has to be evaluated at the beginning of the time interval (prepoint discretization) [38], which corresponds to the Ito prescription, and consequently the mean value of this term vanishes. It is shown in Appendix C that for all values of  $y$  one has that  $|S^{(j)}(y - y_0(\tau))|$  is bounded by  $O(\sqrt{|\varepsilon|})$ ,  $j = 1, 2, 3$ , while  $|I(y - y_0(\tau))|$  is bounded by an exponentially small quantity. If we take then mean value of the above equation, we conclude that  $\langle R_0(y - y_0(\tau))^2 \Theta_{1y} \rangle$  remains bounded everywhere.

#### IV. EVOLUTION OF THE CORE OF THE FRONT

The evolution equation (13) for the core of the front can be written in the form

















